

# Miscellanies of $K^0 - \bar{K}^0$ mixing and $B_K$ \*

Markus Klomfass <sup>a</sup> and Weonjong Lee <sup>b †</sup>

<sup>a</sup>Dept. of Physics, Columbia Univ., New York, NY 10027; Veilchenweg 24, 65201 Wiesbaden, Germany.

<sup>b</sup>IBM, T.J. Watson Research Center, P.O. Box 218, Yorktown Heights, NY 10598, U.S.A.

We have computed  $B_K$ , using two different methods with staggered fermions on a  $16^3 \times 40$  lattice at  $\beta = 5.7$  with two dynamical flavors of a mass 0.01. Using an improved wall source method, we have studied a series of non-degenerate quark antiquark pairs and observed no effect on  $B_K$ , although effects were seen on the individual terms making up  $B_K$ .

## 1. INTRODUCTION

The standard model which is believed to describe our world of hadrons and leptons contains a number of fundamental parameters. The knowledge of hadronic weak matrix elements is crucial to determine these parameters from the experiments. Lattice gauge theory has reached a point that it is capable of calculating hadronic weak matrix elements. Especially, the knowledge of  $B_K$  which describes the neutral  $K$  meson mixing is crucial to narrow the domain of  $V_{td}$  and the top quark mass, which are the fundamental parameters of the standard model.

We have computed  $B_K$  on a  $16^3 \times 40$  lattice at  $\beta = 5.7$  ( $a^{-1} \simeq 2.0$  GeV) with two dynamical flavors of a mass 0.01. The results were obtained over 155 gauge configurations. Our work extends earlier calculations of  $B_K$  and includes experiments with alternative lattice formulations and improved wall source methods. There are two methods to transcribe the continuum weak matrix elements to the lattice with staggered fermions[1,2]: the one spin trace formalism and the two spin trace formalism. The two spin trace formalism (2TR) has been used predominantly for weak matrix element calculations[3]. Recently, the one spin trace formalism (1TR) has been developed to a level which allows it to be used for weak matrix element calculation on the

lattice [1]. We have tried both formalisms to calculate  $B_K$ . The results are compared in this paper. We have studied an improved wall source named *cubic wall source* in order to project out a specific hadronic state exclusively[4]. The results are compared with those of the conventional even-odd wall source. We have looked into the effect of non-degenerate quark antiquark pairs on  $B_K$  and the individual components making up  $B_K$  in detail. From the standpoint of chiral perturbation theory, the effects of non-degenerate valence quark are related to the  $\eta'$  hairpin diagram in (partially) quenched QCD[5]. We interpret our numerical results in terms of chiral perturbation theory.

Preliminary results have already appeared in Ref. [6].

## 2. $K - \bar{K}$ Mixing

In the continuum,  $B_K$  is defined as

$$B_K \equiv \frac{\langle \bar{K}^0 | \bar{s}\gamma_\mu(1 - \gamma_5)d \bar{s}\gamma_\mu(1 - \gamma_5)d | K^0 \rangle}{\frac{8}{3}\langle \bar{K}^0 | \bar{s}\gamma_\mu\gamma_5d | 0 \rangle\langle 0 | \bar{s}\gamma_\mu\gamma_5d | K^0 \rangle}$$

The operator transcription of the continuum  $\Delta S = 2$  operator to the lattice in both one spin trace formalism and two spin trace formalism is explained in Ref. [1]. The numerical results of  $B_K$  calculated in both formalisms are compared in Figure 1. The details of renormalization procedure is given in Ref. [1]. From Figure 1, note that numerical results of the tadpole-improved renormalized  $B_K$  in both formalisms agree with each

\*Talk presented by Weonjong Lee.

<sup>†</sup>Research sponsored in part by the U.S. Department of Energy.

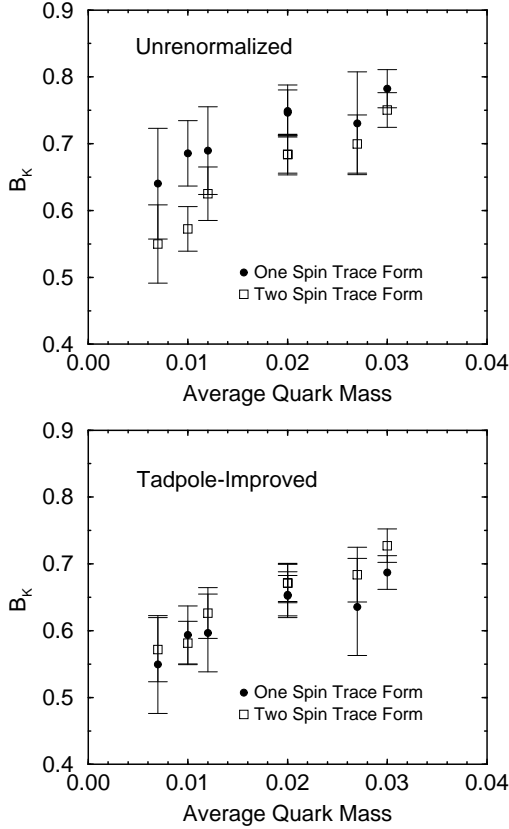


Figure 1. Comparison of  $B_K$  in one spin trace form (filled circle) with  $B_K$  in two spin trace form (empty square). **Top:** unrenormalized  $B_K$ . **Bottom:** tadpole-improved renormalized  $B_K$  at  $\pi/a$  scale. Even-odd wall source is used.

other better than those of unrenormalized  $B_K$ .

Here, we address two important questions on the validity of our approach to  $B_K$ . The higher loop radiative correction of four fermion operators cause the mixing of operators with different spin and flavor structures. The first question is how much the mixing of operators with different flavor structure contributes to our weak matrix measurement at finite lattice spacing non-perturbatively. The second question is how exclusively we can select the pseudo-Goldstone mode using our improved wall source named *cubic wall source*. We have chosen  $((V+A) \otimes S)^{2\text{TR}}$  in order to address the above two questions, where we follow the notation in Ref. [1]. The matrix element

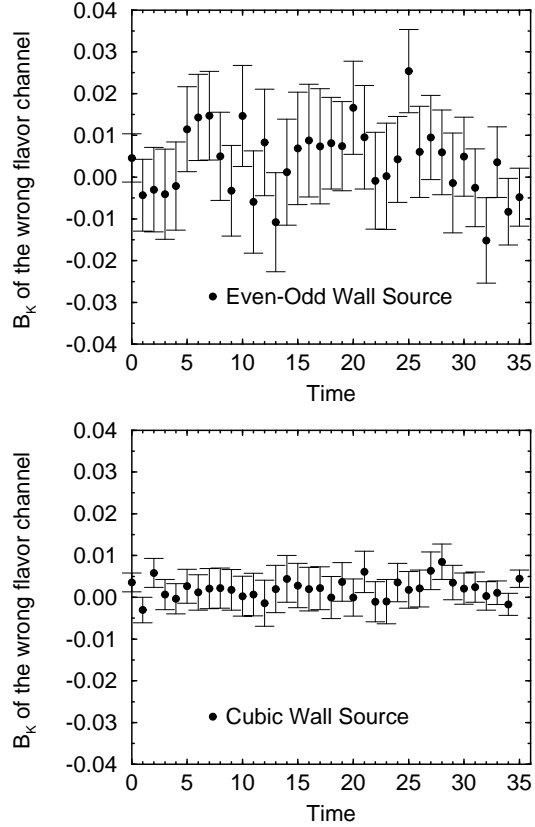


Figure 2. Unrenormalized  $B_K$  of wrong (scalar-like) flavor structure  $((V+A) \otimes S)^{2\text{TR}}$  and of a valence quark mass 0.02 versus the Euclidean time. Calculated in two spin trace form. **Top:** even-odd wall source is used. **Bottom:** cubic wall source is used.

of this operator with  $K$  mesons is supposed to vanish in the continuum limit ( $a \rightarrow 0$ ) of lattice QCD, due to vanishing flavor trace. We present the numerical results of the wrong flavor channel in Figure 2, which tells us that the wrong flavor channel is highly suppressed (within 1% of  $B_K$ ) when cubic source is used. This implies that unwanted mixing of  $((V+A) \otimes S)^{2\text{TR}}$  should be at most 1% of  $B_K$  since it is suppressed by  $\alpha_s/(4\pi)$  as well as by vanishing flavor trace. The small deviation of the wrong flavor channel from zero in Figure 2 tells us how efficiently the improved wall sources suppress contaminations from unwanted hadronic states. In Figure 3, we compare  $B_K$

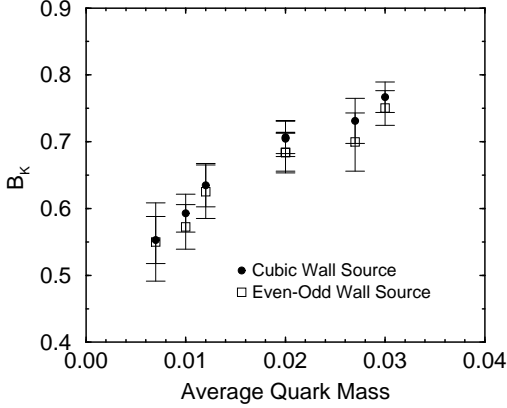


Figure 3. Unrenormalized  $B_K$  vs. average quark mass ( $m_q a$ ): The filled circle (empty square) represents the data of cubic wall source (even-odd wall source). Calculated in the two spin trace formalism.

of cubic wall source with  $B_K$  of even-odd wall source.

Let us jump into the next issue: the effects of non-degenerate quark antiquark pairs on  $B_K$  and its individual components, and their relationship with various chiral logarithms. In our numerical simulation, we have used three degenerate quark antiquark pairs:  $\{(0.01, 0.02, 0.03)\}$ , and four non-degenerate pairs:  $\{(0.004, 0.01), (0.04, 0.02), (0.01, 0.03), (0.01, 0.03)\}$  to produce  $K$  meson state. In order to discuss individual components of  $B_K$  in an organized way, we need to consider a theory with four valence flavors[7]:  $S$  and  $S'$  both with mass  $m_s$  as well as  $D$  and  $D'$  both with mass  $m_d$ . Let  $K^0$  be the  $\bar{S}\gamma_5 D$  pion and  $K'^0$  be the corresponding state with primed quarks ( $\bar{S}'\gamma_5 D'$ ). We define individual components of  $B_K$  as

$$\begin{aligned} \mathcal{V.S.} &\equiv \frac{4}{3} \langle \bar{K}'^0 | \bar{S}'_a \gamma_\mu \gamma_5 D'_a | 0 \rangle \langle 0 | \bar{S}_b \gamma_\mu \gamma_5 D_b | K^0 \rangle \\ B_{V1} &\equiv \langle \bar{K}'^0 | \bar{S}'_a \gamma_\mu D'_b \bar{S}_b \gamma_\mu D_a | K^0 \rangle / \mathcal{V.S.} \\ B_{V2} &\equiv \langle \bar{K}'^0 | \bar{S}'_a \gamma_\mu D'_a \bar{S}_b \gamma_\mu D_b | K^0 \rangle / \mathcal{V.S.} \\ B_{A1} &\equiv \langle \bar{K}'^0 | \bar{S}'_a \gamma_\mu \gamma_5 D'_b \bar{S}_b \gamma_\mu \gamma_5 D_a | K^0 \rangle / \mathcal{V.S.} \\ B_{A2} &\equiv \langle \bar{K}'^0 | \bar{S}'_a \gamma_\mu \gamma_5 D'_a \bar{S}_b \gamma_\mu \gamma_5 D_b | K^0 \rangle / \mathcal{V.S.} \\ B_V &= B_{V1} + B_{V2} \\ B_A &= B_{A1} + B_{A2} \\ B_K &= B_V + B_A \end{aligned}$$

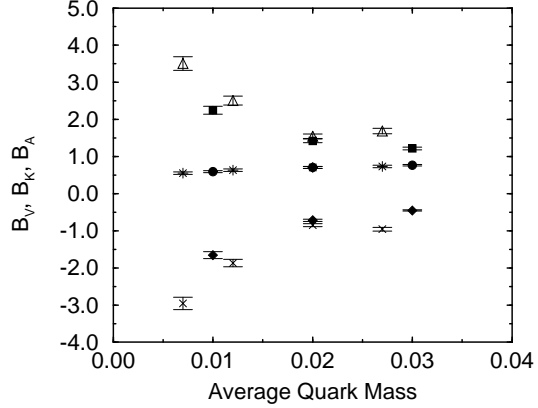


Figure 4. Unrenormalized  $B_K, B_V, B_A$  vs. average quark mass: Calculated using cubic wall source in the two spin trace formalism.  $B_A$ : empty triangle and filled square.  $B_K$ : star and filled circle.  $B_V$ : x and filled diamond. Filled square, circle, and diamond represent degenerate quark antiquark pairs. All other symbols correspond to non-degenerate pairs.

where  $a, b$  represent color indices. Let us summarize chiral perturbation results for the above individual components, the details of which are explained in Ref. [7]. In full QCD chiral perturbation, the one-loop corrections to  $B_{V1}, B_{V2}, B_{A1}$ , and  $B_{A2}$  include a logarithmically divergent term in the chiral limit  $m_K \rightarrow 0$ , which is called an *enhanced chiral logarithms*, and which is absent in  $B_K$ . The enhanced chiral logarithms are not a function of quark mass difference between  $s$  and  $d$  quarks. We present  $B_K, B_V$ , and  $B_A$  data versus quark mass in Figure 4, which illustrates the existence of a divergence in  $B_V$  and  $B_A$  and no divergence in  $B_K$  in the chiral limit.

There are two possible differences between partially quenched or quenched and full QCD. The first difference is that the meson spectrum eigenstates are not same. The second difference comes from  $\eta'$  loops, which can not contribute in full QCD because it is too heavy for chiral dynamics. The hairpin diagram contribution to  $B_K$  and its individual component, which is called “(partially) quenched chiral log”, vanishes in the limit of  $m_s = m_d$ . In other words, (partially) quenched chiral logarithms are functions of quark mass dif-

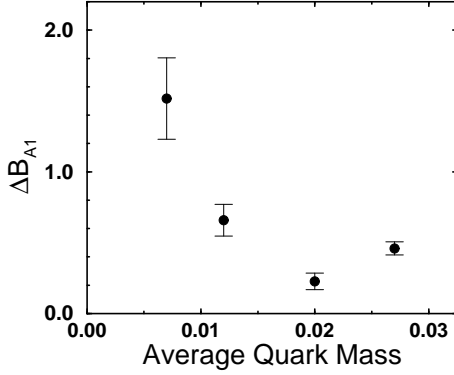


Figure 5.  $\Delta B_{A1}$  vs. average quark mass: Calculated using cubic wall source in the two spin trace formalism.

ference. Since chiral perturbation theory predicts that  $B_{A1}$  has a constant term about 1/3 smaller and an enhanced chiral logarithmic term around 3 times larger than  $B_{A2}$ , we have chosen  $B_{A1}$  as a useful measurement adequate to observe, if present, both enhanced and quenched chiral logarithms. In order to observe the effect of non-degenerate quark antiquark pairs on  $B_{A1}$ , first we fit data of degenerate pairs to obtain  $B_{A1}^{\text{deg}}(m_K)$  and second we subtract those degenerate contributions from non-degenerate data as follows:

$$\Delta B_{A1}(m_K, \epsilon) \equiv \frac{B_{A1}(m_K, \epsilon) - B_{A1}^{\text{deg}}(m_K)}{\epsilon},$$

where  $B_{A1}(m_K, \epsilon)$  is data of non-degenerate quark antiquark pairs and  $\epsilon \equiv (m_s - m_d)/(m_s + m_d)$ . We present  $\Delta B_{A1}$  data in Figure 5, which indicates that there is an additional divergence as a function of  $\epsilon$ . This additional divergence might come from (partially) quenched chiral logarithms or from a finite volume effect. This needs more numerical evidence and further theoretical understanding.

In order to detect the effect of non-degenerate quark antiquarks on  $B_K$ , we follow the procedure similar to  $B_{A1}$  case. First, we fit degenerate data to  $B_K^{\text{deg}}(m_K)$ . Second, we introduce  $\Delta B_K$  as follows:

$$\Delta B_K(m_K) \equiv \frac{B_K(m_K, \epsilon) - B_K^{\text{deg}}(m_K)}{\epsilon^2},$$

where the function is normalized by  $\epsilon^2$  since chiral

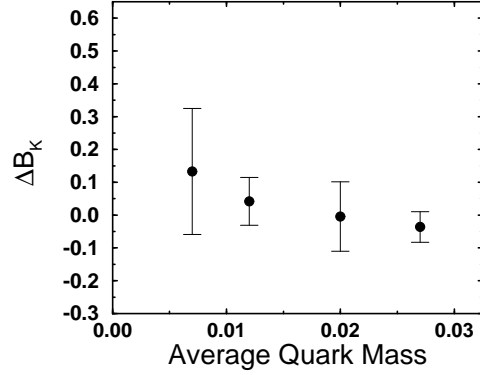


Figure 6.  $\Delta B_K$  versus average quark mass: Calculated using cubic wall source in the two spin trace formalism.

perturbation predicts that leading effect of non-degenerate quark antiquark pairs on  $B_K$  is of order  $\epsilon^2$ . We present the  $\Delta B_K$  data in Figure 6, which illustrates that the non-degenerate quark mass effect is much smaller than our statistical error.

Our best results are unrenormalized  $B_K(m_K) = 0.658(77)$  and tadpole-improved renormalized (N.D.R.)  $B_K(m_K, \mu = \frac{\pi}{a}) = 0.659(63)$ .

One of the authors (W. Lee) wants to express heartfelt gratitude to Prof. N.H. Christ, R.D. Mawhinney, D. Zhu, D. Chen, S. Chandrasukharan, and Z. Dong for their kind help.

## REFERENCES

1. W. Lee and M. Klomfass, Phys. Rev. D **51** (1995) 6426.
2. S. Sharpe *et al.*, Nucl. Phys. **B286** (1987) 253.
3. S. Sharpe, Nucl. Phys. B (Proc. Suppl.) **34** (1994) 403; N. Ishizuka *et al.*, Phys. Rev. Lett. **71** (1993) 24; G. Kilcup, Phys. Rev. Lett. **71** (1993) 1677.
4. M. Fukugita *et al.*, Phys. Rev. D **47** (1993) 4739.
5. S. Sharpe, Phys. Rev. D **46**, (1992) 853.
6. W. Lee and M. Klomfass, Nucl. Phys. B (Proc. Suppl.) **42** (1995) 418.
7. S. Sharpe, Phys. Rev. D **46**, (1992) 3146.